
AFRL-AFOSR-VA-TR-2016-0129

# ANISOTROPIC GRID GENERATION | Deliverables

Daniel Sievenpiper
UNIVERSITY OF CALIFORNIA SAN DIEGO

03/24/2016
Final Report



Air Force Research Laboratory
AF Office Of Scientific Research (AFOSR)/ RTB1
Arlington, Virginia 22203
Air Force Materiel Command

# REPORT DOCUMENTATION PAGE

*Form Approved*
*OMB No. 0704-0188*



**PLEASE DO NOT RETURN YOUR FORM TO THE ABOVE ORGANIZATION.**

| 1. REPORT DATE *(DD-MM-YYYY)* | 2. REPORT TYPE | 3. DATES COVERED *(From - To)* |
|---|---|---|
| 12-03-2016 | Final report | 15-12-2012 - 14-12-2015 |

**4. TITLE AND SUBTITLE**
Anisotropic Grid Generation

**5a. CONTRACT NUMBER**

**5b. GRANT NUMBER**
FA9550-13-1-0014

**5c. PROGRAM ELEMENT NUMBER**

**6. AUTHOR(S)**
Daniel Sievenpiper

**5d. PROJECT NUMBER**

**5e. TASK NUMBER**

**5f. WORK UNIT NUMBER**

**7. PERFORMING ORGANIZATION NAME(S) AND ADDRESS(ES)**
University of California San Diego
5900 Gilman Drive #0407, La Jolla, CA, 92093

**8. PERFORMING ORGANIZATION REPORT NUMBER**

**9. SPONSORING/MONITORING AGENCY NAME(S) AND ADDRESS(ES)**
Air Force Office of Scientific Research

**10. SPONSOR/MONITOR'S ACRONYM(S)**
AFOSR

**11. SPONSOR/MONITOR'S REPORT NUMBER(S)**

**12. DISTRIBUTION/AVAILABILITY STATEMENT**
A

**13. SUPPLEMENTARY NOTES**
none

**14. ABSTRACT**

During this program we have had several major accomplishments. These include finalizing our prior work on simple anisotropic surfaces consisting of discrete regions of homogeneous impedance values, and demonstrating them in the form of several useful structures. Examples include beam shifting structures, and scattering control surfaces. We have also developed a new method for patterning anisotropic surfaces based on defining a set of points which are shifted according to the desired impedance, and then used to define a lattice of cells. The goal of this work is to create smoothly varying inhomogeneous anisotropic impedance surfaces with arbitrary and well-defined impedance profiles that can perform useful functions. We have demonstrated this method in the form of a planar Luneburg lens, and an improved beam shifting structure. We have also developed a method for validating that the pattern of unit cells accurately reproduces the desired impedance function, although this last task is currently still in progress. Our next work is to develop a way to automatically define the starting function for the cell generation algorithm. At that point we will have a full procedure for starting with a desired impedance profile, and validating that the final output produces the intended profile.

**15. SUBJECT TERMS**
Anisotropic Artificial Impedance Surfaces

| 16. SECURITY CLASSIFICATION OF: | | | 17. LIMITATION OF ABSTRACT | 18. NUMBER OF PAGES | 19a. NAME OF RESPONSIBLE PERSON |
|---|---|---|---|---|---|
| a. REPORT | b. ABSTRACT | c. THIS PAGE | | | Daniel Sievenpiper |
| U | U | U | UU | 13 | 19b. TELEPHONE NUMBER *(Include area code)* 858-822-6678 |

Reset

## INSTRUCTIONS FOR COMPLETING SF 298

**1. REPORT DATE.** Full publication date, including day, month, if available. Must cite at least the year and be Year 2000 compliant, e.g. 30-06-1998; xx-06-1998; xx-xx-1998.

**2. REPORT TYPE.** State the type of report, such as final, technical, interim, memorandum, master's thesis, progress, quarterly, research, special, group study, etc.

**3. DATES COVERED.** Indicate the time during which the work was performed and the report was written, e.g., Jun 1997 - Jun 1998; 1-10 Jun 1996; May - Nov 1998; Nov 1998.

**4. TITLE.** Enter title and subtitle with volume number and part number, if applicable. On classified documents, enter the title classification in parentheses.

**5a. CONTRACT NUMBER.** Enter all contract numbers as they appear in the report, e.g. F33615-86-C-5169.

**5b. GRANT NUMBER.** Enter all grant numbers as they appear in the report, e.g. AFOSR-82-1234.

**5c. PROGRAM ELEMENT NUMBER.** Enter all program element numbers as they appear in the report, e.g. 61101A.

**5d. PROJECT NUMBER.** Enter all project numbers as they appear in the report, e.g. 1F665702D1257; ILIR.

**5e. TASK NUMBER.** Enter all task numbers as they appear in the report, e.g. 05; RF0330201; T4112.

**5f. WORK UNIT NUMBER.** Enter all work unit numbers as they appear in the report, e.g. 001; AFAPL30480105.

**6. AUTHOR(S).** Enter name(s) of person(s) responsible for writing the report, performing the research, or credited with the content of the report. The form of entry is the last name, first name, middle initial, and additional qualifiers separated by commas, e.g. Smith, Richard, J, Jr.

**7. PERFORMING ORGANIZATION NAME(S) AND ADDRESS(ES).** Self-explanatory.

**8. PERFORMING ORGANIZATION REPORT NUMBER.** Enter all unique alphanumeric report numbers assigned by the performing organization, e.g. BRL-1234; AFWL-TR-85-4017-Vol-21-PT-2.

**9. SPONSORING/MONITORING AGENCY NAME(S) AND ADDRESS(ES).** Enter the name and address of the organization(s) financially responsible for and monitoring the work.

**10. SPONSOR/MONITOR'S ACRONYM(S).** Enter, if available, e.g. BRL, ARDEC, NADC.

**11. SPONSOR/MONITOR'S REPORT NUMBER(S).** Enter report number as assigned by the sponsoring/ monitoring agency, if available, e.g. BRL-TR-829; -215.

**12. DISTRIBUTION/AVAILABILITY STATEMENT.** Use agency-mandated availability statements to indicate the public availability or distribution limitations of the report. If additional limitations/ restrictions or special markings are indicated, follow agency authorization procedures, e.g. RD/FRD, PROPIN, ITAR, etc. Include copyright information.

**13. SUPPLEMENTARY NOTES.** Enter information not included elsewhere such as: prepared in cooperation with; translation of; report supersedes; old edition number, etc.

**14. ABSTRACT.** A brief (approximately 200 words) factual summary of the most significant information.

**15. SUBJECT TERMS.** Key words or phrases identifying major concepts in the report.

**16. SECURITY CLASSIFICATION.** Enter security classification in accordance with security classification regulations, e.g. U, C, S, etc. If this form contains classified information, stamp classification level on the top and bottom of this page.

**17. LIMITATION OF ABSTRACT.** This block must be completed to assign a distribution limitation to the abstract. Enter UU (Unclassified Unlimited) or SAR (Same as Report). An entry in this block is necessary if the abstract is to be limited.

# Anisotropic Grid Generation

Daniel Sievenpiper, University of California, San Diego

*AFOSR Final Performance Report FA9550-13-1-0014*

## Abstract

During this program we have had several major accomplishments. These include finalizing our prior work on simple anisotropic surfaces consisting of discrete regions of homogeneous impedance values, and demonstrating them in the form of several useful structures. Examples include beam shifting structures, and scattering control surfaces. We have also developed a new method for patterning anisotropic surfaces based on defining a set of points which are shifted according to the desired impedance, and then used to define a lattice of cells. The goal of this work is to create smoothly varying inhomogeneous anisotropic impedance surfaces with arbitrary and well-defined impedance profiles that can perform useful functions. We have demonstrated this method in the form of a planar Luneburg lens, and an improved beam shifting structure. We have also developed a method for validating that the pattern of unit cells accurately reproduces the desired impedance function, although this last task is currently still in progress. Our next work is to develop a way to automatically define the starting function for the cell generation algorithm. At that point we will have a full procedure for starting with a desired impedance profile, and validating that the final output produces the intended profile.

## Introduction

The interaction between electromagnetic waves and objects can be defined entirely by the surface impedance of those objects. This controls the scattering behavior and thus the radar cross-section, and it also controls surface wave propagation which determines antenna coupling parameters, interference between co-located electronic systems, and all other aspects of electromagnetic interaction. Thus, defining the surface impedance is important for controlling how such systems behave. This has traditionally been accomplished with layered materials, resistance cards, magnetic radar absorbing materials, and other such treatments. It has also been accomplished with periodic structures such as frequency selective surfaces. For the past several years, the field of meta-surfaces has been continually evolving. Beginning with the high impedance surface in 1999, the field has expanded to include holographic surfaces, which have been used to create conformal antennas and cloaking structures. These provide a much simpler approach than other work in metamaterials, because they are built using an electrically thin structure which can be fabricated using printed circuit technology.

It is now recognized that anisotropy can provide even greater control over the propagation of surface waves, and the scattering of incoming plane waves. A classic example is the soft and hard surfaces that were studied several decades ago, which can be used to enhance or suppress TM or TE surface waves depending on the direction of propagation. Such structures can also be implemented as artificial impedance surfaces, whereby they can be much thinner and simpler

to fabricate. Several simple examples of applications for anisotropic surfaces will be described below. The difficulty with creating arbitrary anisotropic surfaces is that they require elongated unit cells to create high anisotropy. Because such cells do not fit into a regular square or hexagonal grid, regions with different primary directions of anisotropy cannot be smoothly or easily connected, as shown in figure 1. As a result, all of the initial work with such patterns involved discrete regions of homogeneous impedance. We have now developed a new technique for producing arbitrary and isotropic impedance services, which is the primary topic of this report. We have demonstrated that such structures can be useful for performing certain electromagnetic functions, and we have fabricated and tested several examples. Our present work is on validating that the patterns generated by this technique produce the intended impedance profile.

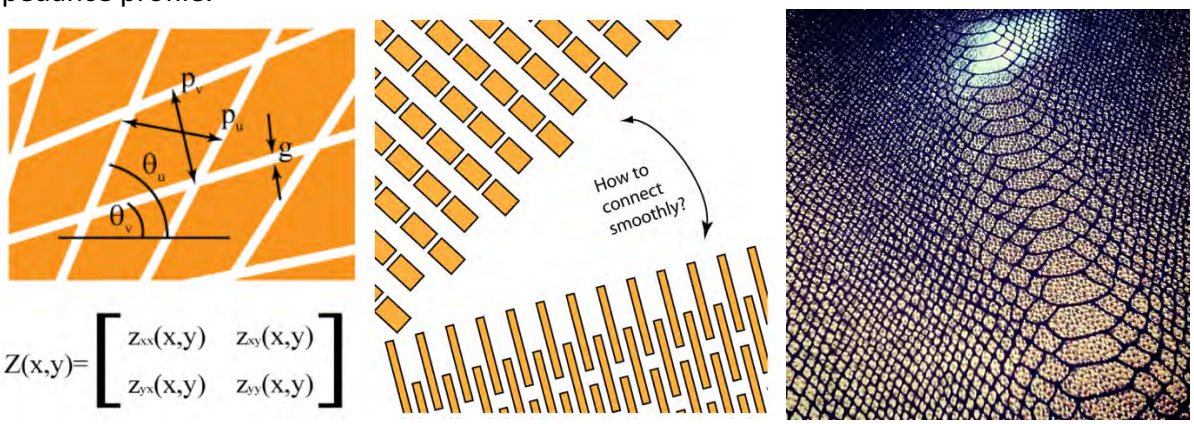


*Figure 1. An example of a simple pattern to produce an anisotropic impedance surface, which can be described by an impedance tensor. The impedance is largely controlled by the length of the cells along each direction. The difficulty identified on the center panel is that highly anisotropic regions with different primary directions cannot be smoothly or easily connected. The goal of this work is to produce the electromagnetic equivalent of snake skin, pictured at right, with smoothly varying cells of different sizes and orientations.*

## Background and Applications

A variety of anisotropic impedance surface structures have been studied in the past, and several examples are shown in figure 2. These include the original holographic anisotropic surface which was studied by the author, as well as similar structures that have been studied by other groups. The common theme of these structures is that the individual unit cells have some kind of anisotropy, either in the form of slices with varying angles, or having different capacitances in different directions. Regardless of the approach, the result is the same and the impedance along a given direction is a result of the sheet capacitance in that direction, which generally relates to the length of the unit cell and the density of gaps in that direction. The limitation of these approaches is that the cells must have an aspect ratio close to one, such as squares, circles, or hexagons. To create highly anisotropic impedance surfaces, highly elongated cells are needed. However, as discussed above, these are difficult to form into arbitrary patterns because they cannot be arranged on a simple grid that still allows for arbitrary and varying angles.

*Figure 2. Examples of previous anisotropic surfaces include the original holographic tensor impedance surface created by the author (left), a similar structure studied by Stefano Maci (center), and another variant studied by Tony Grbic (right).*

As one approach to creating anisotropic unit cells, we have explored a variation on the classic mushroom shape, which is shown in figure 3. Adding a conductive via increases the available impedance range significantly. However, it also substantially reduces the bandwidth. The structure shown in figure 3 is a compromise, where the via is present but capacitively connected to the patch. The patch is also elongated to produce an anisotropic surface impedance. The result is that this structure can have both broad bandwidth and also a wide range of impedance values. The drawback of the structure is that the basic unit cell is still a square or rectangle, and thus it can only be arranged on a regular grid, forbidding the potential of smoothly varying arbitrary patterns.

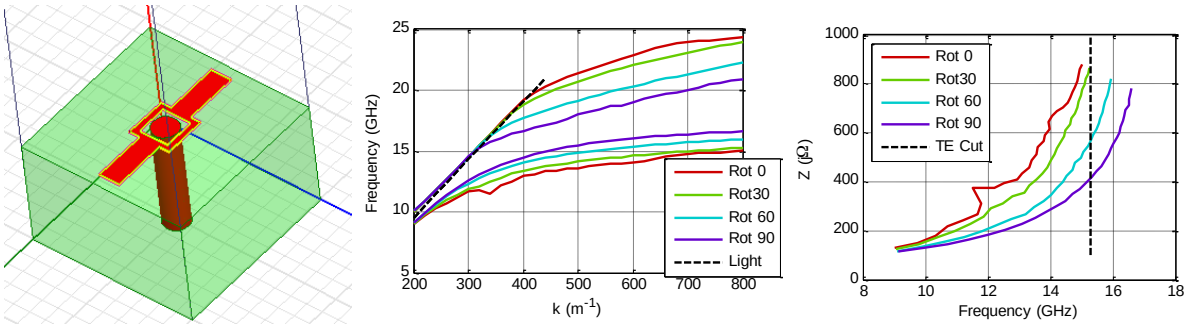


*Figure 3. A broadband anisotropic cell design consists of an elongated patch and a capacitively coupled via. The capacitive coupling allows the surface to retain the wide impedance range, while increasing the bandwidth.*

Nonetheless, this unit cell type has proven the potential of highly anisotropic unit cells for practical applications. One example is shown in figure 4. This is a small section of the interface between two different regions of anisotropic impedance surface based on the unit cell type shown in figure 3. The entire structure was much larger than this small section, roughly 12 x 18". This sample allowed us to test refraction at a boundary between two anisotropic impedance surfaces, and also to demonstrate the beam shifting approach, and techniques for guiding surface waves around obstacles. As shown in the figure, a surface wave will refract both upon entering the surface, and upon passing into a second impedance surface with a different primary direction. When the interface between the two surfaces is illuminated directly, the incoming wave is split into two beams, and can thus avoid a scattering object that would otherwise be in the way. This can be used for example to reduce scattering by holes or apertures in the skin of an aircraft, or to control the direction of propagation of waves along the metal body.

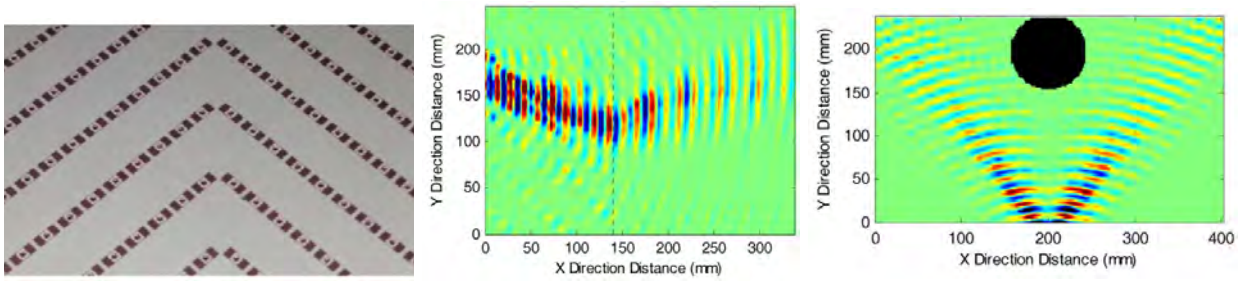


*Figure 4. A beam shifter example based on a boundary between two anisotropic impedance surfaces with different primary directions. A surface wave is refracted at the boundary between the two surfaces. When the boundary is illuminated directly, the beam is split in two, and thus avoids a scattering obstacle placed on the seam.*

As a more direct demonstration of using anisotropic surfaces for scattering control, we have also explored creating artificial edges, which can be used to mitigate scattering by both vertical and horizontal polarization if the artificial edge is created between anisotropic impedance surfaces. These boundaries can be thought of as soft or hard surfaces, and they represent the limit when the impedance is very high in one direction, and very low in the other direction. The ideal soft or hard surface would be an electric conductor along one direction and a magnetic conductor along the other direction. The difference between soft versus hard is merely a rotation by 90°. In our case, we implement the soft and hard boundaries as anisotropic impedance surfaces that are oriented in orthogonal directions. Figure 5 shows such a geometry, with the boundary between the two surfaces oriented at a diagonal along the rectangular structure. Waves with vertical polarization are scattered at the trailing edge of an electric conductor, whereas horizontal polarization is scattered by the leading edge. The two cases are reversed for a magnetic conductor. Thus, the geometry shown in figure 5 causes scattering for both vertical and horizontal polarization to occur along the diagonal, rather than at either the leading or trailing edge boundary. As shown in the two plots, the primary reflection peak is shifted by 20° in both cases, and the backscattered beam is reduced by roughly 10 dB.

The demonstration in figure 5 still involved anisotropic surfaces that are homogeneous, and relied on a sharp boundary between regions to provide the scattering control. The next demonstration involves a smoothly varying surface, although not one that takes advantage of our new patterning technique. In this case, the unit cells are simply small rectangular patches which are oriented in various directions, shown in figure 6. The patches are gradually rotated to change the primary direction of anisotropy. The goal of this structure is too smoothly steer the wave away from the diagonal edge, to affect the scattering from that edge. If the wave impinges up on the edge at a different direction, phase matching at the edge will dictate that the reflected wave will be directed to somewhere else, and the scattering due to that edge will be reduced. As shown in the figure, the peak corresponding to scattering from the diagonal edge is effectively eliminated by the smoothly varying anisotropic impedance surface, and the energy is likely spread over other angles. The next step in this work is to develop techniques that enable substantially higher anisotropy with smoothly varying impedance functions.

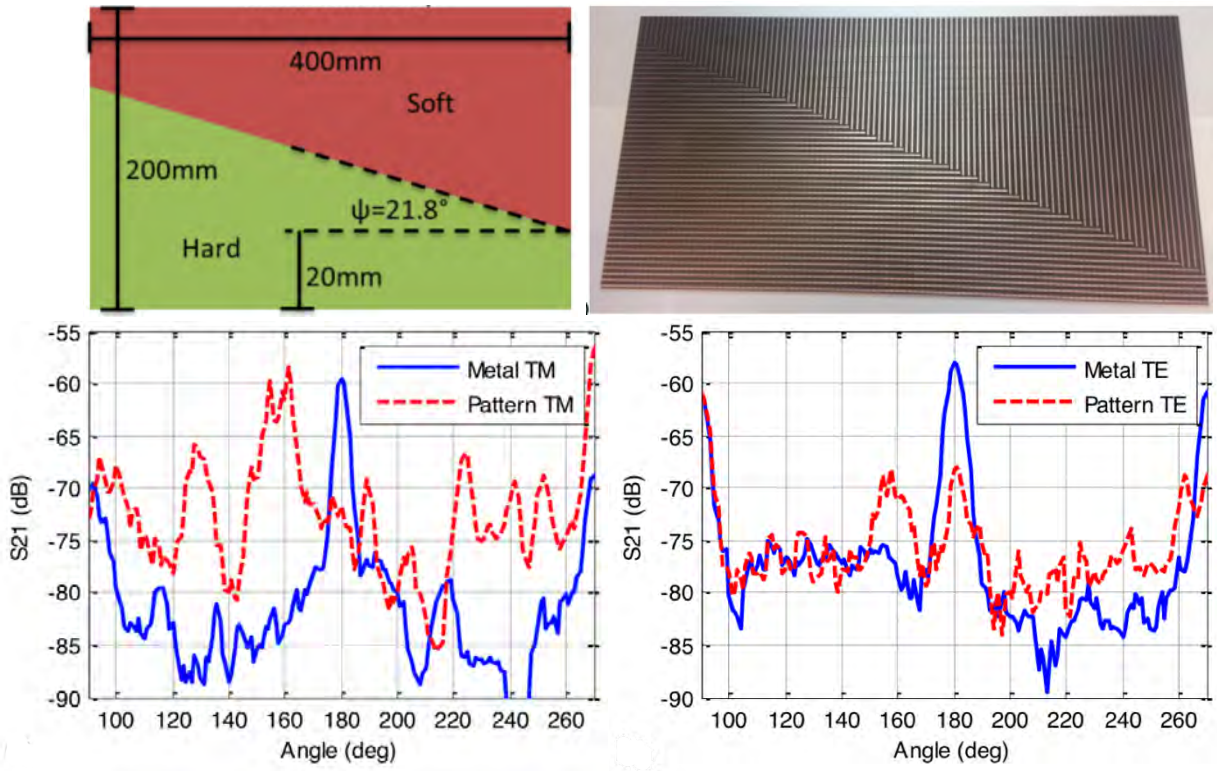


*Figure 5. Scattering control demonstrating using a false edge. The edge divides two different anisotropic impedance surfaces that behave as soft or hard surfaces, and have opposite scattering properties for vertical and horizontal polarization. Both polarizations are scattered at the false edge, thus shifting the primary scattering peak by 20 degrees. The backscattered component is also reduced by 10 dB in both cases.*

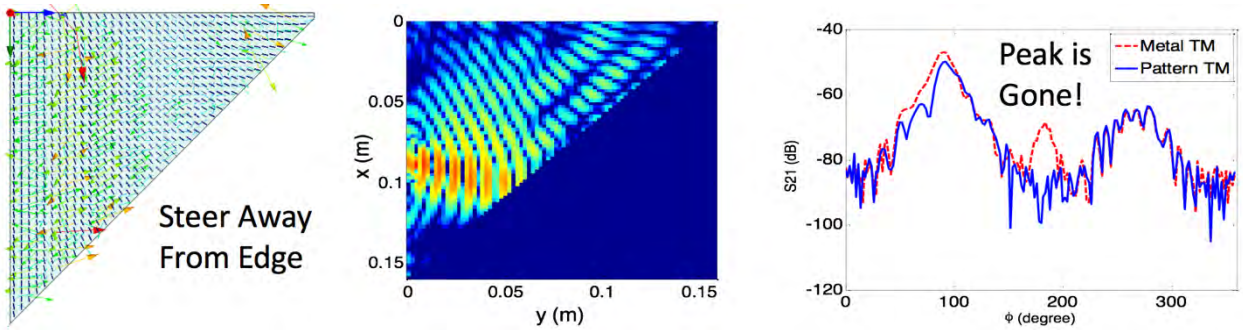


*Figure 6. Scattering control using a smoothly varying impedance surface, implemented as an array of rectangular patches that are oriented at an arbitrary angle. The patches are slowly rotated as a function of position across the surface to provide a smoothly varying impedance function, which is chosen to guide the incoming wave away from the diagonal edge. The scattering component due to that edge is eliminated as shown in the panel at right.*

In order to allow for larger impedance values, greater anisotropy, and more arbitrary patterns, we have set out to develop a way to move from regular patterns such as shown above toward nonuniform lattices. These present both new challenges and new opportunities, as will be discussed below. During this research several approaches were tried, and the one discussed here is that which was found to be the most successful, and which are are continuing with as part of our current research.

## Cell Generation Technique

The heart of our new pattern and technique is a method for defining cells which have arbitrary size, shape, and orientation. After exploring a variety of other approaches based on intersecting lines, variable point density clouds, and other ideas, we focused on the method describe here which has so far been successful. The basic idea, illustrated in figure 7, is to begin with a function that describes the desired surface impedance. For example, assume one would like to create an impedance surface with a local maximum. A set of points represents the starting grid, which may be square or exit. The points are then moved from their original positions according to the gradient of the starting function. Moving the points inward would create a local minimum, because it would result in smaller cells in the center. Moving the points outward, as the negative of the gradient, results in larger cells in the center and a local maximum. The final pattern of points is then said into a cell generation algorithm based on the Voronoi approach.

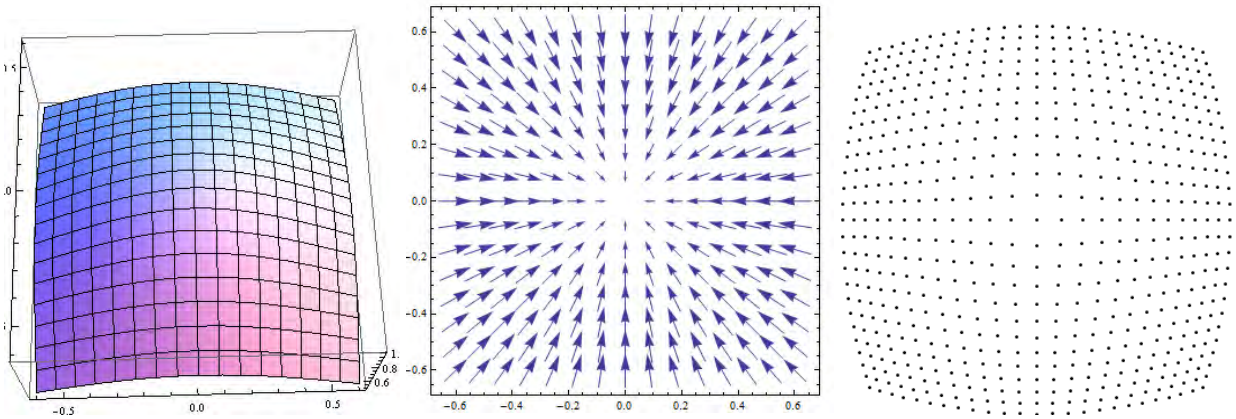

*Figure 7. The cell generation technique involves taking the gradient of a starting function, and using that to shift a set of points which are initially arranged on a regular grid. The points become the centers of the unit cells defined by the Voronoi method.*

A Voronoi diagram is a method of dividing space into regions based on a set of points. It is well-established in the fields of mathematics and physics, and it is the same approach used to generate Brillouin zone diagrams. In short, lines are drawn between each pair of points, and the envelope of those lines defines a cell around each point. Thus, the cell boundaries represent the midpoint between every pair of neighboring points. Starting with this basic diagram, unit cells must then be created. A cell is initially defined by a set of line segments. To create a fixed gap with between neighboring cells, those segments must be moved inward by half the desired gap width. Then a new set of vertices is defined by the intersection of the shifted line segments. Because the cell boundaries are oriented at various angles, care must be taken to ensure that glitches are not created in the set of the vertices. In addition, if two initial vertices are closer together than the intended gap with, it is possible that one vertex may be eliminated, and this must be accounted for in the code. Each of these issues has been sorted out, and we now have a robust code that is capable of taking a set of points and generating a set of unit cells having a fixed gap width between them. And example of this approach is shown in figure 8. The resulting cells have a wide range of shapes which depend on the starting function and the initial array of points. Using a hexagonal grid of points instead of a square grid also results in different cell shapes. In general, the cells will range from rectangles to diamonds and hexagons, and anything in between. Each of these cases has also been studied under a previous program.

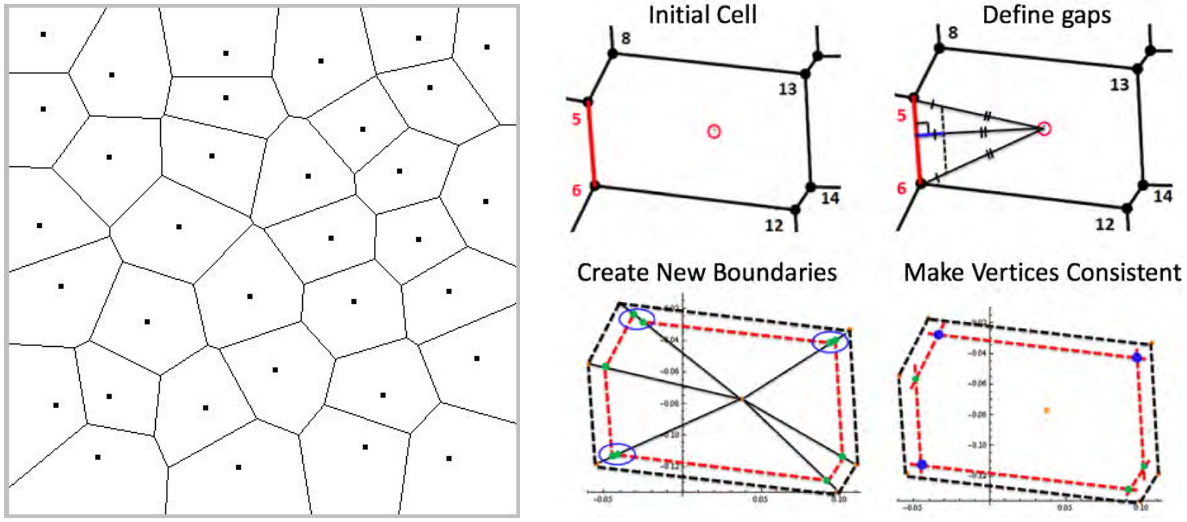


*Figure 8. The Voronoi cell patterning technique involves generating a Voronoi diagram around the set of shifted points, and then creating cells with a fixed gap width based on the line segments, which are shifted to create a new set of vertices.*

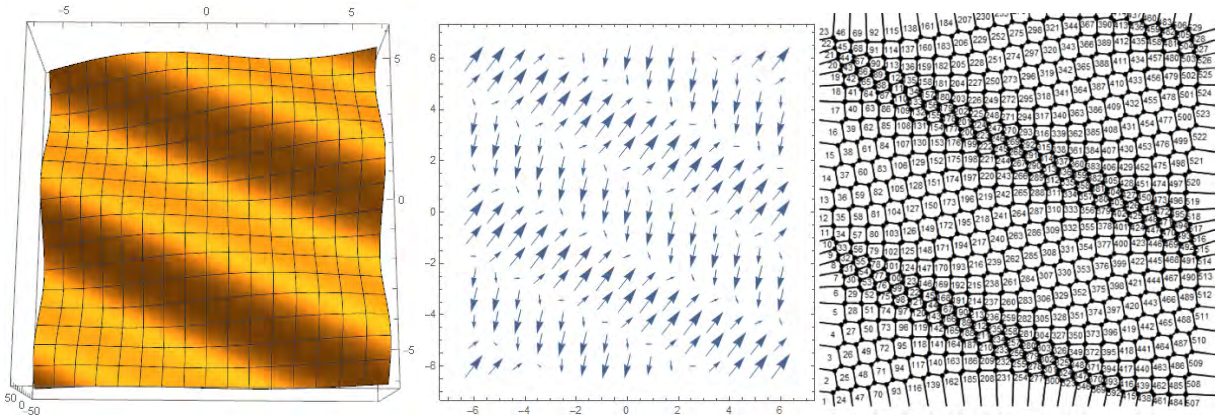

*Figure 9. An example of a sinusoidally varying starting function, and the set of unit cells generated from it.*

Figure 9 shows a more complex example, with a two-dimensional sheet that varies sinusoidally at an arbitrary angle. The gradient of the sheet is first determined, and then the point shifting and Voronoi cell generation technique is applied, creating a set of cells that vary in a sinusoidal manner, matching the starting function. If the points are spread out or compressed along one direction but not the other, the result is an anisotropic surface because the Voronoi technique ensures that the cell boundaries are midway between each point and its neighbors.

This method is capable of producing a wide range of patterns that have practical applications. Several examples, illustrated in figure 10, include cells with the variable shape, variable length, and variable orientation. In addition, it is clearly possible to produce cells that are highly anisotropic, and are arranged in arbitrary patterns that would not be possible using any previously existing pattern and techniques that we are aware of. Thus, this essentially demonstrates that we have achieved the initial goal of this program, to produce a method of creating new kinds of patterns automatically which have relevance to smoothly varying anisotropic impedance surfaces.

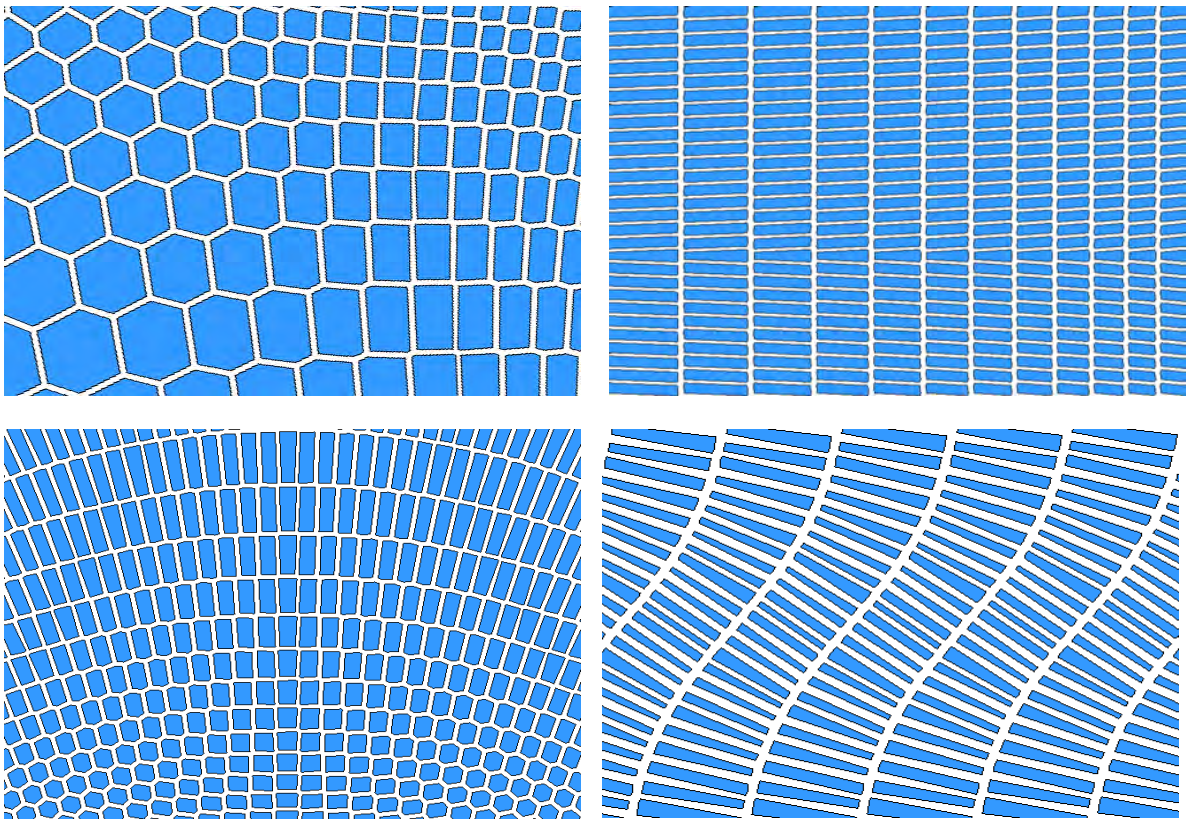

*Figure 10. Various patterns can be created from the point shifting and Voronoi cell generation technique. These examples show, from upper left to lower right, smoothly varying cell shape, smoothly varying cell size, smoothly varying cell angle, and in the final panel an extreme and highly variable example of an anisotropic structure that is useful as a beam shifting structure. These demonstrate that we have achieved the goal of this program to develop a patterning method that can produce smoothly varying and highly anisotropic impedance surfaces*

## Example Structures

In order to demonstrate that these anisotropic impedance surfaces can perform useful functions, we have developed several examples to illustrate their capabilities. The first is a simple planar Luneburg lens, which does not actually require anisotropy, but does require a smoothly varying impedance function. The Luneburg lens requires a refractive index that varies from 2 at the center to 1 at the edge according to a well-known function which is available in the literature. It is traditionally constructed with shells having various indices of refraction. Planer versions have also been developed using a similar approach. Or aim with this demonstration is to show that our point shifting and Voronoi cell generation technique is capable of producing a smoothly varying impedance function which can generate the expected results. Since the structure is well known, it provides a suitable example. Figure 11 shows a traditional planer Luneburg lens constructed with rings of various impedance values. It also shows a portion of a lens constructed using our technique. The cells are chosen specifically to be large in this case so that they are visible, and the actual structure involved smaller cells.

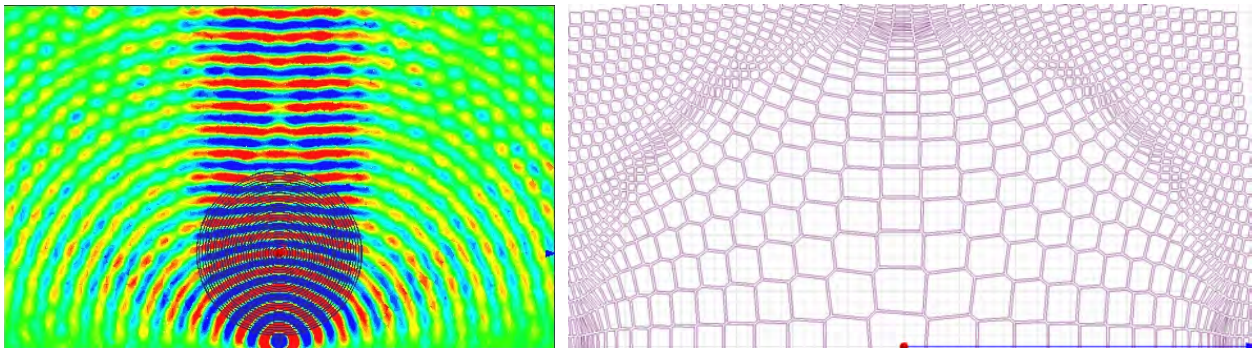

*Figure 11. Luneburg lens example for the purpose of demonstrating that the smoothly varying unit cells can perform a useful function. The left panel shows a traditional planar Luneburg lens created by shells of various impedance values, and the right panel shows a section of a lens created using our patterning technique.*

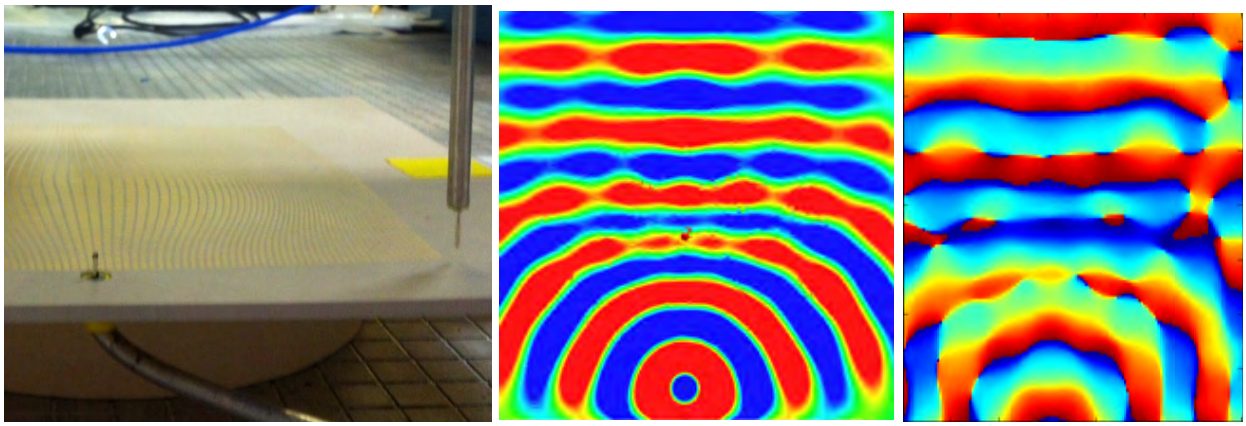

*Figure 12. Measurements (left) of the fabricated planar Luneburg lens indicate that the simulations (center) are validated by the measured data (right).*

In figure 12, the measurement set up is seen. The planar Luneburg lens was illuminated by a point source at one edge. The function of this lens is to transform that point source to a plane wave on the opposite side of the lens. To measure its radiation properties, we scan a second probe above the surface and measure the field. By performing this two-dimensional scan, we can plot the electric field over the surface of the lens and demonstrate that it forms a plane wave on the other side. The measured data correlates well with the simulations, verifying that the lens performs as expected.

Although the lens requires a smoothly Bering impedance function, it does not actually require anisotropy. For this reason, we have also developed a smoothly varying version of the beam shifter described earlier. It contains elongated unit cells that are twisted at an angle a long one line, and they cause the surface wave to bend in the direction of the twist. The simulations shown in figure 13 indicate that the structure should perform the beam shifting task. The next step is to build and measure this structure, and this effort is currently underway on the continuation of this program.

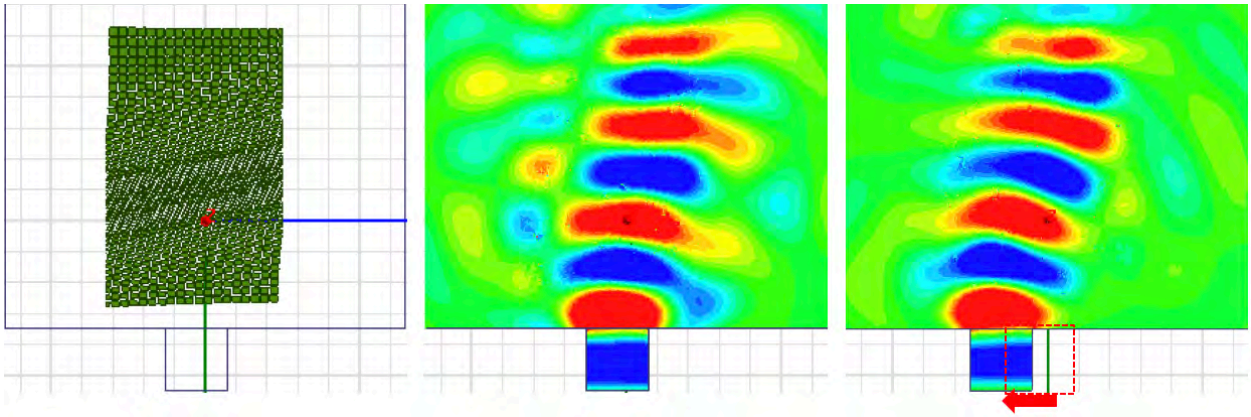

*Figure 13. Beam shifter built using a smoothly varying impedance surface implemented using our patterning method. The simulations indicate that it should work as expected. The third panel shows improved performance by offsetting the feed.*

## Validation Approach

In order to verify that the unit cells produced using our patterning technique accurately recreate the desired impedance function, we must develop a method to extract an effective surface impedance from a pattern of cells. The basic idea is illustrated in figure 14. Beginning with a refractive index as a function of position, which corresponds to the starting function in our technique, we generate a set of cells. We then extract parameters for each of the cells, and translate them into an effective impedance on a cell by cell basis. This effective impedance is the patterned back onto the surface in the form of an abstract impedance boundary, and simulated to determine if the indicated impedance function accurately represents the intended function. This effort has now begun using a technique to be described below. The one missing piece of this method is that we do not yet have a way to translate from the desired impedance function to the starting function, and that is the next step in this work.

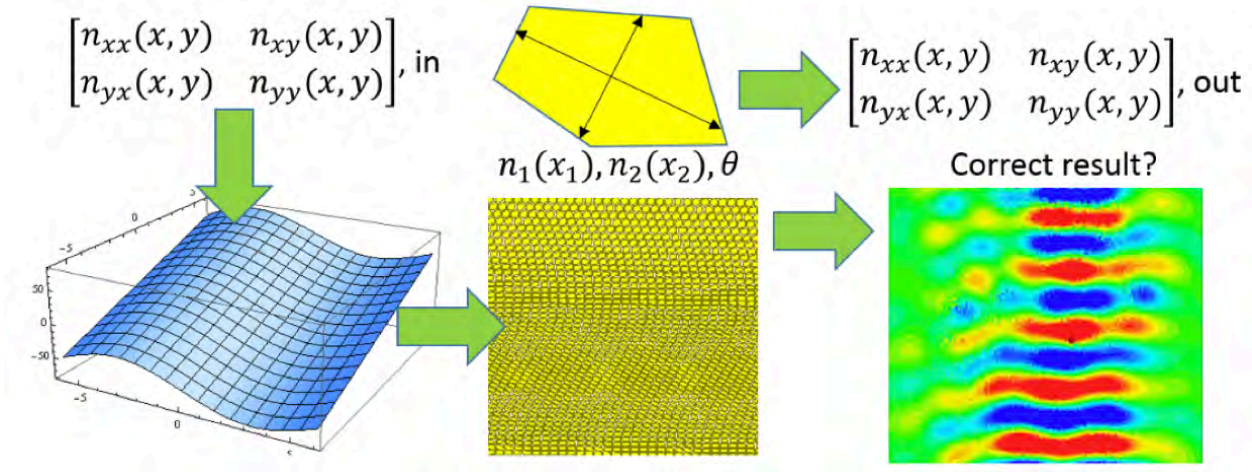


*Figure 14. Our approach to validating our cell generation method is to develop an effective impedance tensor that can be extracted from the properties of each unit cell. This impedance tensor can be mapped back onto the surface, and simulations of this surface can be compared to the intended performance. The impedance extraction technique is based on the moment of inertia method, described below.*

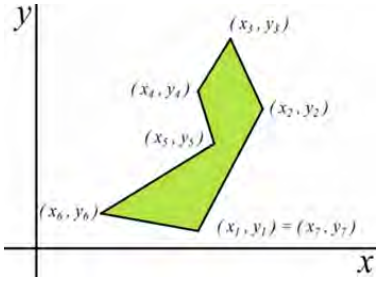


$$I_x = \frac{1}{12}\sum_{i=1}^{i=N}(y_i^2 + y_i y_{i+1} + y_{i+1}^2)(x_i y_{i+1} - x_{i+1} y_i)$$

$$I_y = \frac{1}{12}\sum_{i=1}^{i=N}(x_i^2 + x_i x_{i+1} + x_{i+1}^2)(x_i y_{i+1} - x_{i+1} y_i)$$

$$I_{xy} = \frac{1}{24}\sum_{i=1}^{i=N}(x_i y_{i+1} + 2x_i y_i + 2x_{i+1} y_{i+1} + x_{i+1} y_i)(x_i y_{i+1} - x_{i+1} y_i)$$

*Figure 15. The moment of inertia method is based on the idea that the impedance of a set of unit cells is related largely to the length of the cells in each direction, similar to the inertia tensor in mechanics. Fortunately, it is straightforward to calculate the moment of inertia for an arbitrary shape, as shown here.*

The effect of surface impedance extraction method is based on the concept of moment of inertia, borrowed from mechanics. The inspiration for this method is as follows. We knew that the impedance of each cell is largely a function of the length of that cell in a given direction. In other words, elongated cells have a high impedance in the long direction, and a low impedance in the short direction. This is similar to the idea of the moment of inertia an elongated object, which is greater in the long direction than in the short direction. Thus, we theorize that it is possible to extract an effective length and width for a rectangular patch that is representative of a patch having any arbitrary shape. Furthermore, we theorize that the moment of inertia of the two patches would be similar, or would be related by a simple function. Fortunately, it is possible to calculate the moment of inertia for any arbitrary shape consisting of line segments, illustrated in figure 15. The task of generating an effective impedance profile for a set of cells then consists of calculating the moment of inertia of each cell, translating that to an impedance tensor which is calculated based on effective rectangular cells, and then applying that impedance tensor to a map of the surface.

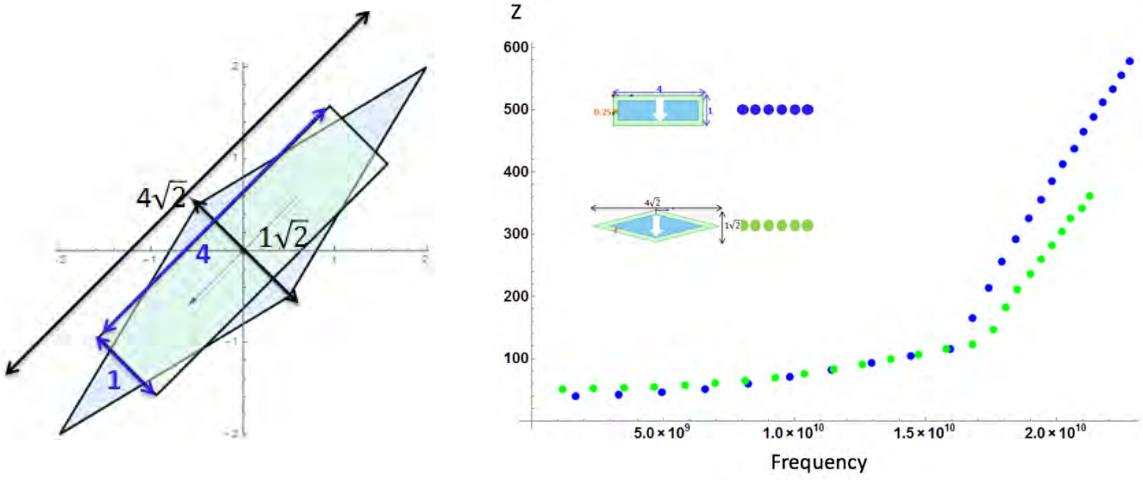


*Figure 16. One of the cell types studies is the diamond shaped cell. The impedance matches that of the effective rectangular cell calculated from the moment of inertia method up to a cutoff frequency beyond which the TE mode interferes.*

The first step in creating this validation procedure is to compare the impedance tensor of a periodic lattice of cells having various shapes to the impedance tensor of effective rectangular cells created from the moment of inertia method. Figure 16 and figure 17 show two examples, for an elongated diamond, and a hexagon. Various other examples have also been studied, and

the results are similar to what is shown here for these two cases. Both cases show an excellent match between the impedance of the actual unit cell and the impedance of the effective rectangular cell based on the moment of inertia method. Both cell types show the same trend, and accurate recreation of the impedance function based on the effective rectangular cell up to a certain frequency, followed by a sharp deviation. This deviation corresponds to the expectation of a TE wave, which mixes with the TM wave in anisotropic impedance surfaces. Thus, we can safely use the rectangular cells as a substitute for the real cells below this cut off frequency.

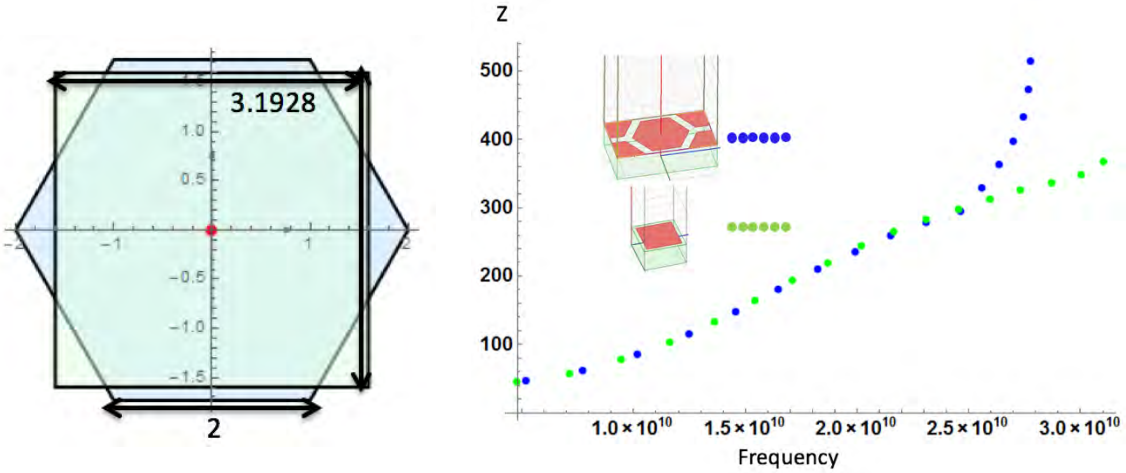


*Figure 17. The hexagon type cell is also similar to its effective rectangular cell up to a cutoff frequency where the TE mode appears. Other cell types show similar behavior. Thus, we can use the effective rectangular cell to determine the impedance tensor for arbitrary cell shapes.*

The next step in this work is to develop an automatic extraction code which will generate a set of impedance tensors based on each unit cell in the array, and then apply those impedance tensors to the cell area to allow us to perform a new simulation to verify that the effect of impedance matches the intended value. This will also require us to develop a way to translate the desired impedance function to the starting function, and both of these efforts are currently underway.

## Future Work

The overall goal of this program is to develop a way to control the flow of surface currents on complex metallic objects. This begins with a set of desired surface currents described in terms of power flow and wave vector, or phase profile. This may be derived from desired scattering properties for example, or desired coupling values between two nearby antennas. We need to develop a way to translate this desired surface current profile into an impedance or refractive index profile. We then need to develop a way to translate this impedance profile to a set of unit cells. This has been partially developed under this program, as described in this report, because we now have a way to generate arbitrary unit cell patterns which are non-uniform and highly anisotropic. The missing piece in this effort is a way to translate from the impedance profile to the starting function for generating the unit cells, however, that work is currently underway. The final piece is to validate the performance of the unit cells, and that work is also currently underway. The long-term vision is to be able to create a surface that produces any desired

scattering profile in a controllable and well-defined way. In addition, another goal is to increase bandwidth, reduce thickness, and overall improved performance. In the future, this may be possible with active surfaces such as non-Foster loaded surfaces. Preliminary investigation of these surfaces is also underway.

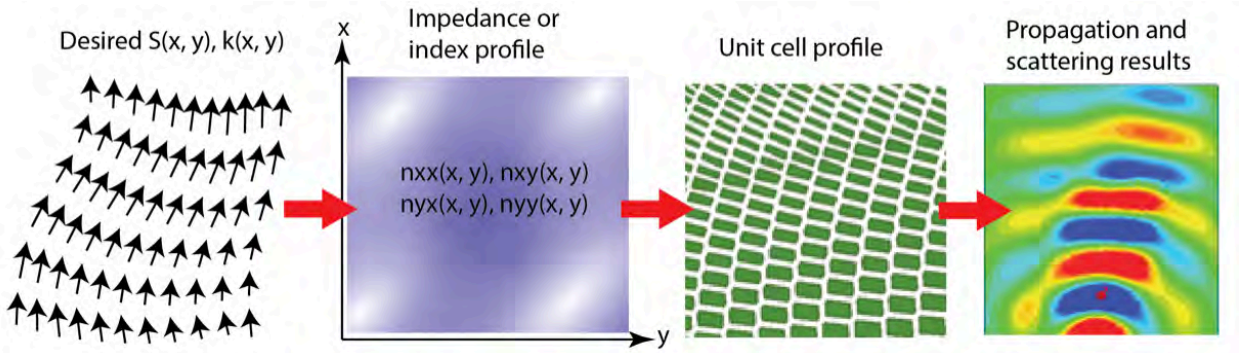


*Figure 18. Future work involves translating a desired surface current profile into an impedance profile. We have already developed a method for creating a set of unit cells, but we need to determine a way to translate the desired impedance function into the starting function. We are also developing methods to validate the impedance profile, as described above.*

1.

**1. Report Type**

Final Report

**Primary Contact E-mail**

**Contact email if there is a problem with the report.**

dsievenpiper@eng.ucsd.edu

**Primary Contact Phone Number**

**Contact phone number if there is a problem with the report**

858-822-6678

**Organization / Institution name**

University of California San Diego

**Grant/Contract Title**

**The full title of the funded effort.**

Anisotropic Grid Generation

**Grant/Contract Number**

**AFOSR assigned control number. It must begin with "FA9550" or "F49620" or "FA2386".**

FA9550-13-1-0014

**Principal Investigator Name**

**The full name of the principal investigator on the grant or contract.**

Daniel Sievenpper

**Program Manager**

**The AFOSR Program Manager currently assigned to the award**

Arje Nachman

**Reporting Period Start Date**

12/15/2012

**Reporting Period End Date**

12/14/2015

**Abstract**

During this program we have had several major accomplishments. These include finalizing our prior work on simple anisotropic surfaces consisting of discrete regions of homogeneous impedance values, and demonstrating them in the form of several useful structures. Examples include beam shifting structures, and scattering control surfaces. We have also developed a new method for patterning anisotropic surfaces based on defining a set of points which are shifted according to the desired impedance, and then used to define a lattice of cells. The goal of this work is to create smoothly varying inhomogeneous anisotropic impedance surfaces with arbitrary and well-defined impedance profiles that can perform useful functions. We have demonstrated this method in the form of a planar Luneburg lens, and an improved beam shifting structure. We have also developed a method for validating that the pattern of unit cells accurately reproduces the desired impedance function, although this last task is currently still in progress. Our next work is to develop a way to automatically define the starting function for the cell generation algorithm. At that point we will have a full procedure for starting with a desired impedance profile, and validating that the final output produces the intended profile. The missing piece in this effort is a way to translate from the impedance profile to the starting function for generating the unit cells, however, that work is currently underway. The final piece is to validate the performance of the unit cells, and that work is also currently underway. The long-term vision is to be able to create a surface that produces any desired scattering

profile in a controllable and well-defined way. In addition, another goal is to increase bandwidth, reduce thickness, and overall improved performance.

**Distribution Statement**

**This is block 12 on the SF298 form.**

Distribution A - Approved for Public Release

**Explanation for Distribution Statement**

**If this is not approved for public release, please provide a short explanation. E.g., contains proprietary information.**

**SF298 Form**

**Please attach your SF298 form. A blank SF298 can be found here. Please do not password protect or secure the PDF**
**The maximum file size for an SF298 is 50MB.**

AFD-070820-035.pdf

**Upload the Report Document. File must be a PDF. Please do not password protect or secure the PDF . The maximum file size for the Report Document is 50MB.**

final report.pdf

**Upload a Report Document, if any. The maximum file size for the Report Document is 50MB.**

**Archival Publications (published) during reporting period:**

**Changes in research objectives (if any):**

none

**Change in AFOSR Program Manager, if any:**

none

**Extensions granted or milestones slipped, if any:**

none

**AFOSR LRIR Number**

**LRIR Title**

**Reporting Period**

**Laboratory Task Manager**

**Program Officer**

**Research Objectives**

**Technical Summary**

**Funding Summary by Cost Category (by FY, $K)**

| | Starting FY | FY+1 | FY+2 |
|---|---|---|---|
| Salary | | | |
| Equipment/Facilities | | | |
| Supplies | | | |
| Total | | | |

**Report Document**

**Report Document - Text Analysis**

**Report Document - Text Analysis**

**Appendix Documents**

## 2. Thank You

**E-mail user**